Journal of Thermal Analysis and Calorimetry, Vol. 57 (1999) 797-806

HEAT OF FORMATION FOR $LiM_yMn_{2-y}O_4$ (M=Co, Cr, Li, Mg, Ni) SPINEL SOLID SOLUTION

R. Yamaguchi, H. Ikuta and M. Wakihara

Department of Chemical Engineering, Tokyo Institute of Technology, 2-12-1 O-okayama
Meguro-ku, Tokyo, 152-8552 Japan

Abstract

The enthalpy of formation for $LiM_yMn_{2-y}O_4$ (M=Co, Cr, Li, Mg, Ni) was measured by a Tian-Calvet type high temperature isothermal microcalorimeter. The standard enthalpy of formation for $LiMn_2O_4$ at 876 K was evaluated to be $\Delta H_f^o=-1404.2\pm6.4$ kJ mol^{-1}. The partial substitution of Co and Ni for Mn decreased the absolute ΔH_f^o value, while that of Cr and Mg for Mn increased the absolute ΔH_f^o value. In the case of the partial substitution of Li for Mn, no marked change in ΔH_f^o could be observed.

Keywords: high temperature combustion calorimetry, in-situ high-temperature powder XRD, lithium manganese spinel oxide, TG-DTA measurements

Introduction

Rechargeable lithium-ion batteries using intercalation compound $LiCoO_2$ as the positive electrode and carbon as the negative electrode have been studied intensively in this last decade [1, 2]. However $LiCoO_2$ is unstable in view of the thermodynamics, cobalt is a relatively rare and expensive transition metal, so that instead, spinel-type lithium manganese oxide $LiMn_2O_4$ has attracted a great deal of research because of its economic and environmental advantages.

In the $LiMn_2O_4$ spinel structure, the oxygen atoms form a face-centered cubic packing and occupy 32e sites of the $Fd\bar{3}m$ space group. The Li ions are located at the tetrahedral 8a sites and the manganese ions occupy the octahedral 16d sites. The octahedral 16c sites remain empty.

Unfortunately $LiMn_2O_4$ has a rapid capacity fade upon cycling [3]. To overcome this problem, $LiM_yMn_{2-y}O_4$ (M=Co, Cr, Li, Mg, Ni), in which Mn ions were partially substituted by other cations M, offered better cycle performance [4, 5]. It seems that the structural stabilization by partial substitution of other cation M for Mn in $LiMn_2O_4$ has induced the improvement of cycle performance.

Tarascon *et al.* [3] have shown that $Li_{1+x}Mn_{2-x}O_4$ lost oxygen at elevated temperature using TG measurement and oxygen deficient samples had inferior electrochemical properties. It has been shown by Thackeray *et al.* [6] that the phase transition of lithium manganese spinel oxides was caused by loss of oxygen and lithia (Li_2O) at elevated temperature. However, the main reason of the phase transition has not been clarifed.

1418–2874/99/ $ 5.00

Akadémiai Kiadó, Budapest
Kluwer Academic Publishers, Dordrecht

In this study, the heat effect of the preparation of $LiMn_2O_4$ and $LiM_yMn_{2-y}O_4$ are directly measured by a drop calorimetry in a Tian-Calvet type high temperature isothermal microcalorimeter in order to discuss the structural stability in view of the thermodynamics. From the measured heat, we calculate the enthalpies of formation for $LiMn_2O_4$ and $LiM_yMn_{2-y}O_4$. Furthermore, we report in-situ high-temperature powder X-ray diffraction data of the parent $LiMn_2O_4$ and $LiM_{1/6}Mn_{11/6}O_4$ (M=Co, Cr) samples together with thermogravimetric analysis (TG) data and differential thermal analysis (DTA) data of these spinel oxides.

Experimental

$LiM_yMn_{2-y}O_4$ (M=Co, Cr, Li, Mg, Ni) samples were prepared by reacting a stoichiometric mixture of Li_2CO_3 (99.9%, Soekawa Chemical Co., Ltd.), $MnCO_3$ (99.9%, Soekawa Chemical Co., Ltd.), Co_3O_4, Cr_2O_3, MgO and NiO in calorimeter. Co_3O_4 and NiO were prepared by decomposing oxalate at low temperature, in the same way, Cr_2O_3 were prepared from hydroxide, and MgO from carbonate. This procedure gave these oxides with smaller particle size and higher reactivity compared with commercialized reagents which have relatively larger particle size. These samples prepared in calorimeter are named as ‘cCo6’, ‘cCr6’, etc. depending on the substituted metals for Mn and substituted amount y (Table 1).

Table 1 Summary of preparation conditions

Sample	Composition	Starting materials	Conditions
cMn6	$LiMn_2O_4$	$LiCO_3$, $MnCO_3$	876 K, 1 h, in calorimeter
cCo6	$LiCo_{1/6}Mn_{11/6}O_4$	Li_2CO_3, $MnCO_3$, Co_3O_4	876 K, 1 h, in calorimeter
cCr6	$LiCr_{1/6}Mn_{11/6}O_4$	Li_2CO_3, $MnCO_3$, Cr_2O_3	876 K, 1 h, in calorimeter
cLi6	$Li_{7/6}Mn_{11/6}O_4$	Li_2CO_3, $MnCO_3$	876 K, 1 h, in calorimeter
cMg6	$LiMg_{1/6}Mn_{11/6}O_4$	Li_2CO_3, $MnCO_3$, MgO	876 K, 1 h, in calorimeter
cNi6	$LiNi_{1/6}Mn_{11/6}O_4$	Li_2CO_3, $MnCO_3$, NiO	876 K, 1 h, in calorimeter
fMn6	$LiMn_2O_4$	Li_2CO_3, Mn_2O_3	1023 K, 96 h, in furnace
fCo6	$LiCo_{1/6}Mn_{11/6}O_4$	Li_2CO_3, Mn_2O_3, $CoC_2O_4{\cdot}2H_2O$	1023 K, 72 h, in furnace
fCr6	$LiCr_{1/6}Mn_{11/6}O_4$	Li_2CO_3, Mn_2O_3, Cr_2O_3	1023 K, 72 h, in furnace
fMg6	$LiMg_{1/6}Mn_{11/6}O_4$	Li_2CO_3, Mn_2O_3, MgO	1023 K, 96 h, in furnace
fNi6	$LiNi_{1/6}Mn_{11/6}O_4$	Li_2CO_3, Mn_2O_3, $NiC_2O_4{\cdot}2H_2O$	1023 K, 72 h, in furnace

For the measurement of reaction heat, we used a Tian-Calvet type high temperature microcalorimeter [7, 8]. In this calorimeter the thermal effect was detected as an electrical output with a thermocouple. In order to obtain the enthalpy change, the electrical signal was magnified by a microvolt amplifier and integrated using a personal computer. Calibration of the calorimeter was performed by dropping a spherical gold at room temperature into the calorimeter at 876 K. The calibrated heat content remained constant within ±0.4% when the measured heat was above 5 J. The mixture of starting materials of about 20 mg was pressed into pellets, and the pellets at room temperature were dropped into calorimeter at 876 K. It took l h to measure the heat of reaction under air flow (l.5 $cm^3\ s^{-1}$). Heat content of the starting materials, which was needed for calculation, were estimated from the measured heat. Other thermodynamic enthalpy data which were not able to measure were cited from the reference data [9]. The obtained compounds were identified by powder X-ray diffractometry (XRD) using CuK_α radiation (RINT-2500, Rigaku Co., Ltd).

$LiMn_2O_4$ and $LiM_yMn_{2-y}O_4$ (y=1/6, M=Co, Cr, Mg, Ni) samples for TG-DTA and in-situ high-temperature X-ray diffraction measurements were prepared by reacting a stoichiometric mixture of Li_2CO_3, Mn_2O_3 prepared from $MnCO_3$ at 873 K for 48 h and $CoC_2O_4{\cdot}2H_2O$ (reagent grade, Kanto Chemical Co., Ltd) or Cr_2O_3 (reagent grade, Yoneyama Chemical Industries Ltd.), MgO prepared from $4MgCO_3{\cdot}Mg(OH)_2{\cdot}3H_2O$ at 973 K for 48 h, $NiC_2O_4{\cdot}2H_2O$ (reagent grade, Kanto Chemical Co., Ltd) in air at 1023 K for 72 h ($LiMn_2O_4$, M=Cr, Ni) or for 96 h (M=Co, Mg). These samples are denoted as fMn6, fCo6, fCr6, fMg6 and fNi6, respectively (Table 1).

The decomposition process of $LiMn_2O_4$ and $LiM_{1/6}Mn_{11/6}O_4$ (M=Co, Cr, Mg, Ni) was analyzed in air from room temperature to 1473 K by TG and DTA techniques (Sinku-Riko TGD-9600). The scan rate was 5 K min^{-1} on heating and cooling.

The structure of $LiMn_2O_4$ and $LiM_{1/6}Mn_{11/6}O_4$ (M=Co, Cr) at high temperature were analyzed by means of in-situ high-temperature powder X-ray diffraction. Samples heated in air were held for 300 s at each temperature (973, 1123 and 1253 K) before collecting the diffraction data. The data were collected over the diffraction angle 2θ between 10 and 120° in a step of 0.04° under the condition, 55 kV and 220 mA. Rietveld analysis was performed by using the computer program RIETAN [10].

Results and discussion

The single phase region of $LiM_yMn_{2-y}O_4$ (M=Co, Cr, Li, Mg, Ni) prepared in the calorimeter (876 K, l h) fell in the range $0 \leq y \leq 0.33$ for M=Co, Cr, Mg, $0 \leq y \leq 0.17$ for M=Li and $0 \leq y \leq 0.5$ for M=Ni, respectively. According to Born-Haber cycle, the enthalpy of formation ΔH_f^o for $LiMn_2O_4$ is evaluated as shown in Fig. l. Similarly, considering the enthalpy of formation data for Co_3O_4, Cr_2O_3, Li_2CO_3, MgO and NiO from literature [9], the enthalpy of formation ΔH_f^o for $LiM_yMn_{2-y}O_4$ (M=Co, Cr, Li, Mg, Ni) is also evaluated at 876 K. Detailed values are shown in Table 2, and plotted *vs.* substituted metal composition y (Fig. 2). The standard enthalpy of formation for $LiMn_2O_4$ was estimated to be –1404.2±6.4 kJ mol^{-1}. The partial substitution of Co and Ni for Mn decreased the absolute ΔH_f^o value, while that of Cr and Mg for Mn increased the absolute ΔH_f^o value. In the case of the partial substitution of Li for Mn, no marked change in ΔH_f^o could be observed.

Figure 3(a) and (b) shows the TG and DTA plots of fMn6 and fCo6, when heated from room temperature to 1473 K and cooled to room temperature. In both TG curves, two steps of mass loss can be seen. In DTA curves on heating, an endothermic peak can be observed around the temperature at which the second mass loss in

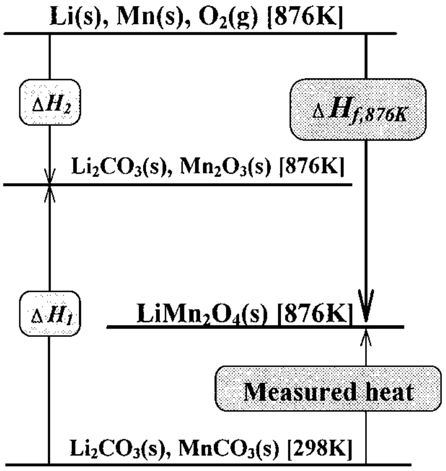

Fig. 1 Born-Haber cycle to evaluate the standard enthalpy of formation for $LiMn_2O_4$
ΔH_1: Heat content of starting materials (298 K–876 K)
ΔH_2: The enthalpy of formation for starting materials (876 K)

Table 2 The standard enthalpy of formation at 876 K for $LiMn_2O_4$, $LiM_yMn_{2-y}O_4$ (M=Co, Cr, Li, Mg, Ni) and related starting materials $LiMn_2O_4$: ΔH_f^o=–1404.2±6.4 kJ mol^{-1}

y in $LiM_yMn_{2-y}O_4$	M=Co/	M=Cr/	M=Li/	M=Mg/	M=Ni/
			kJ mol^{-1}		
0.042	–1398.2±2.7		–1417.6±2.9	–1404.5±1.5	
0.083	–1382.5±1.9	–1411.6±4.4	–1411.3±3.0	–1410.9±1.3	–1363.9±5.1
0.111	–1377.2±2.2	–1414.3±6.7	–1415.6±3.2	–1418.3±0.8	–1358.0±6.1
0.167	–1378.4±3.1	–1424.4±3.0	–1409.1±1.8	–1422.5±1.2	–1327.6±3.6
0.2	–1367.0±1.2	–1430.7±5.8		–1428.5±1.7	–1318.9±8.6
0.25				–1429.7±1.3	
0.333	–1347.2±1.8	–1436.1±4.3		–1444.1±3.6	–1264.3±3.5
0.5					–1172.7±5.1
Li_2CO_3	–1215.9*	Co_3O_4	–891.0*	MgO	–600.6*
Mn_2O_3	–956.7*	Cr_2O_3	–1139.7*	NiO	–239.7*

* The standard enthalpy of formation at 876 K cited from [9]

TG occurred. However, no peaks can be seen near the temperature at first mass loss occurred. Same curves were observed for fCr6, fMg6 and fNi6. Table 3 summarized the temperature at which the mass loss occurred and DTA peak emerged. As for the sample fMn6, there was a second peak at 1328 K where no mass loss could be observed in TG curve. The present TG-DTA data for $LiMn_2O_4$ are quite similar to the results reported by Thackeray *et al.* [6].

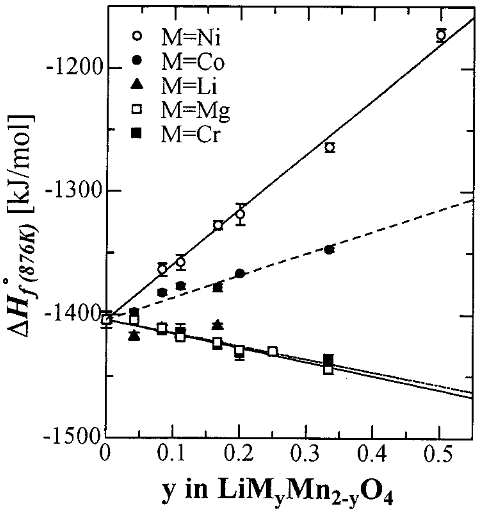

Fig. 2 The standard enthalpy of formation at 876 K for $LiM_yMn_{2-y}O_4$ (*M*=Mn, Co, Cr, Li, Mg, Ni)

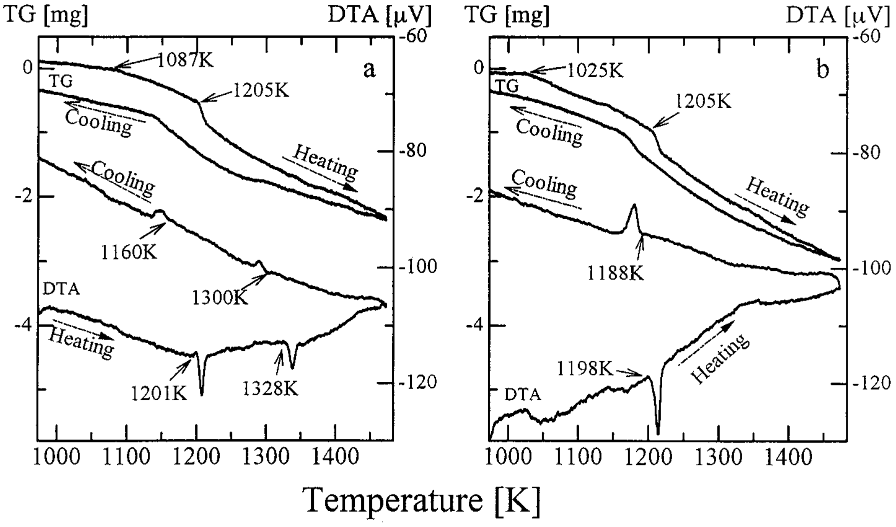

Fig. 3 TG-DTA plots of (a) $LiMn_2O_4$ and (b) $LiCo_{1/6}Mn_{11/6}O_4$ measured under air flow

Figures 4, 5 and 6 show the series of powder XRD patterns for fMn6, fCo6 and fCr6 taken both at elevated temperature and at room temperature after cooling. All the samples still maintained spinel structure at 973 K. When samples were heated to 1123 K, the Li_2MnO_3 phase with monoclinic symmetry, in which all the Mn ions are tetravalent, existed in the chart of fMn6 and fCo6. At 1253 K, the peaks of Li_2MnO_3 phase existed for all the samples and became larger than that at 1123 K (Table 4). In

Table 3 Starting temperature at which mass loss occurred in TG curves and endothermic peaks emerged in DTA curves

Sample	TG (on heating)		DTA (on heating)	
	1st mass loss/K	2nd mass loss/K	1st peak/K	2nd peak/K
fMn6	1087	1205	1201	1328
fCo6	1025	1205	1198	–
fCr6	1116	1211	1213	–
fMg6	995	1194	1199	–
fNi6	1038	1177	1165	–

powder XRD patterns after cooled to room temperature, we could see some peaks belong to Li_2MnO_3 phase and Mn_3O_4 (hausmannite) or $M_zMn_{3-z}O_4$ (M=Co, Cr) phase in which Mn are partially substituted by other cation M besides the peaks of parent $LiMn_2O_4$ or $LiM_{1/6}Mn_{11/6}O_4$. Because the lattice parameter for hausmannite phases in fCo6 and fCr6 varied with substituted metals M (M=Co, Cr). The value z in $M_zMn_{3-z}O_4$ has been estimated to be 0.4 for M=Co and 0.2 for M=Cr by comparing the lattice parameter with the reported value in Ref. [11–13].

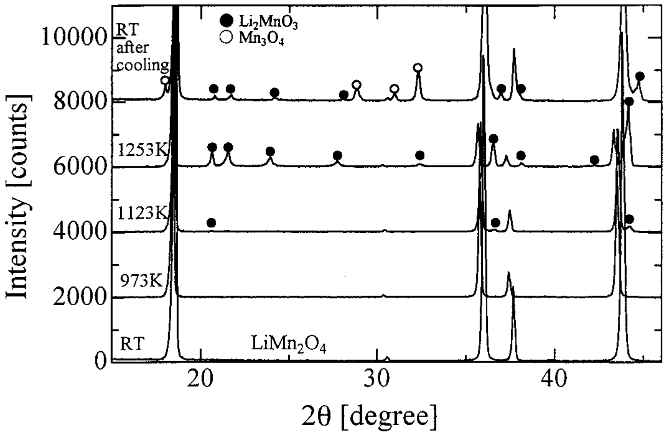

Fig. 4 In-situ high-temperature powder XRD patterns of $LiMn_2O_4$ recorded at room temperature (RT) to 1253 K and at RT after cooling

Combining the TG-DTA and XRD data for the parent $LiMn_2O_4$ and $LiM_{1/6}Mn_{11/6}O_4$, the first mass loss in TG curves has been associated with the removal of oxygen from the surface of the spinel oxides. The second mass loss in TG curves has been originated from a phase transition of a part of both $LiMn_2O_4$ and $LiM_{1/6}Mn_{11/6}O_4$ to monoclinic Li_2MnO_3. This decomposition process for $LiMn_2O_4$ can be expressed as follows,

$$2LiMn_2O_4 \rightarrow Li_2MnO_3 + Mn_3O_4 + 1/2O_2 \quad (1)$$

From the amount of monoclinic phase in powder XRD patterns at 1123 and 1253 K (Table 3), the order of the decomposition along Eq. (1) is fCo6, fMn6 and fCr6. The similar behavior on mass loss in substituted spinels has been obtained in our previous work on the dependence of oxygen partial pressure at 1023 K [14].

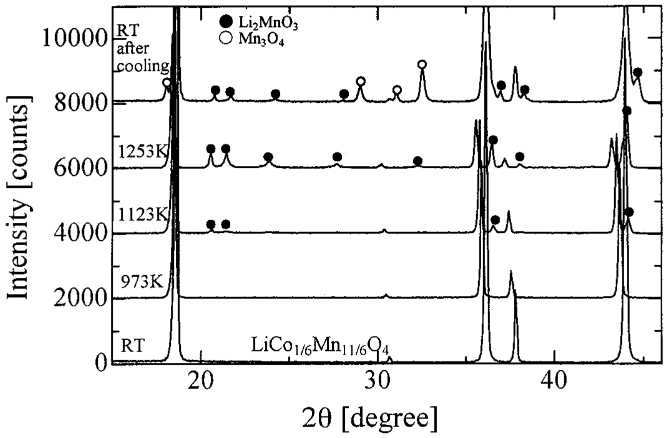

Fig. 5 In-situ high-temperature powder XRD patterns of $LiCo_{1/6}Mn_{11/6}O_4$ recorded at room temperature (RT) to 1253 K and at RT after cooling

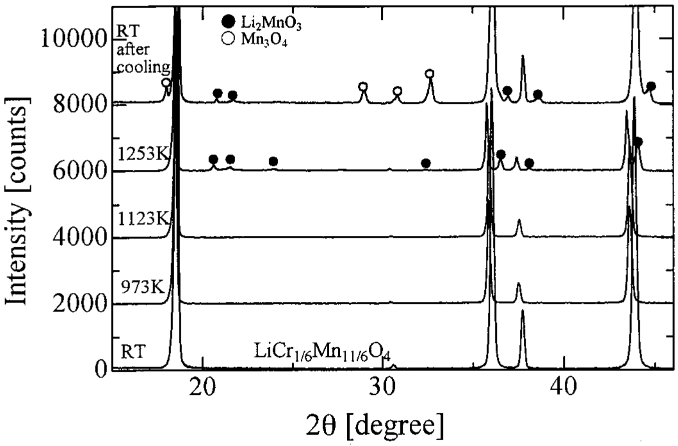

Fig. 6 In-situ high-temperature powder XRD patterns of $LiCr_{1/6}Mn_{11/6}O_4$ recorded at room temperature (RT) to 1253 K and at RT after cooling

Figure 7 shows a relationship between enthalpy of formation ΔH_f^0 on $LiM_yMn_{2-y}O_4$ (cMn6, cCo6, cCr6, cMg6 and cNi6) and the decomposition temperature (fMn6, fCo6, fCr6, fMg6 and fNi6). ΔH_f^0 seems to be in proportion to decomposition temperature except for the ΔH_f^0 of M=Mg. Because Mg belongs to typical elements, it may have somewhat different character compared with other transition metals Co, Cr and Ni. Although the stability of the structure can not be discussed with formation

Table 4 Results of Rietveld refinements from in-situ high-temperature powder XRD data

		At 1253 K		After cooled to room temperature	
		mass ratio/ wt%	lattice parameters/ Å	mass ratio/ wt%	lattice parameters/ Å
fMn6	$LiMn_2O_4$ (cubic)	38.3	*a*=8.3629(2)	80.1	*a*=8.2405
	Mn_3O_4 (tetragonal)			14.2	*a*=5.7610(5), *c*=9.449(1)
	Li_2MnO_3 (monoclinic)	61.7	*a*=4.9987(4), *b*=8.6250(6) *c*=9.7995(7), β=99.40(5) deg.	15.7	*a*=4.923(2), *b*=8.523(3) *c*=9.619(4), β=99.75(5) deg.
fCo6	$LiCo_{1/6}Mn_{11/6}O_4$	39.1	*a*=8.3815(2)	73.4	*a*=8.2191(2)
	$Co_{2/5}Mn_{13/5}O_4$			19.3	*a*=5.7433(6), *c*=9.371(1)
	Li_2MnO_3	60.9	*a*=5.0063(2), *b*=8.6663(5) *c*=9.8154(6), β=99.44(4) deg.	7.3	*a*=4.923(3), *b*=8.528(4) *c*=9.629(6), β=99.71(6) deg.
fCr6	$LiCr_{1/6}Mn_{11/6}O_4$	62.1	*a*=8.3371(2)	82.3	*a*=8.2287(1)
	$Cr_{1/5}Mn_{11/6}O_4$			13.2	*a*=5.7842(5), *c*=9.309(1)
	Li_2MnO_3	37.9	*a*=5.0017(5), *b*=8.6563(8) *c*=9.8078(9), β=99.50(9) deg.	4.5	*a*=4.927(2), *b*=8.526(4) *c*=9.639(6), β=99.66(5) deg.

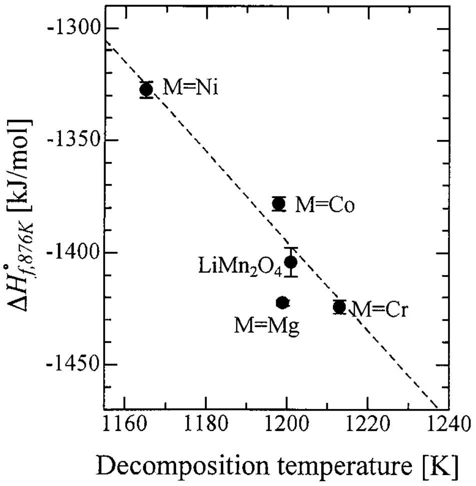

Fig. 7 Relationship between decomposition temperature and the enthalpy of formation of $LiM_{1/6}Mn_{11/6}O_4$ (*M*=Mn, Co, Cr, Mg, Ni)

enthalpy only, it seems to be various factors to determine the enthalpy of formation, bonding energy, the energy for decomposition and electron configuration etc.

Conclusions

The standard enthalpy of formation for $LiMn_2O_4$ at 876 K was estimated to be $\Delta H_f^o=-1404.2\pm6.4$ kJ mol^{-1}. The partial substitution of Cr and Mg for Mn increased the absolute ΔH_f^o value, while that of Co and Ni for Mn decreased the absolute ΔH_f^o value. The partial substitution of Li for Mn showed no marked change in ΔH_f^o value.

The thermal stability of $LiMn_2O_4$ and $LiM_{1/6}Mn_{11/6}O_4$ (*M*=Co, Cr, Mg, Ni) were studied by TG-DTA and in-situ high-temperature powder X-ray diffraction measurement. These samples were partially decomposed to monoclinic Li_2MnO_3 at high temperature. Moreover, there seems to be proportional relationship between ΔH_f^o and decomposition temperature on samples in which Mn were substituted by transition metals Co, Cr, Ni.

References

1 E. Plichta, S. Slane, M. Uchiyama, M. Salomon, D. Chua, W. B. Ebner and H. W. Lin, J. Electrochem. Soc., 136 (1989) 1865.
2 H. F. Gibbard, J. Power Sources, 26 (1989) 81.
3 J. M. Tarascon, W. R. McKinnon, F. Coowar, T. N. Bowmer, G. Amatucci and D. Guyomard, J. Electrochem. Soc., 141 (1994) 1421.
4 Li Guohua, H. Ikuta, T. Uchida and M. Wakihara, J. Electrochem. Soc., 143 (1996) 178.
5 R. J. Gummow, A. de Kock and M. M. Thackeray, Solid State Ionics, 69 (1994) 59.

6 M. M. Thackeray, M. F. Mansuetto, D. W. Dees and D. R. Vissers, Mater. Res. Bull., 31 (1996) 133.

7 M. Nishio, N. Kuwata, H. Hinode, M. Wakihara and M. Taniguchi, Thermochim. Acta, 88 (1985) 101.

8 N. Kuwata, M. Nishio, H. Hinode and M. Wakihara, Thermochim. Acta, 109 (1986) 181.

9 Thermodynamic databases 'MALT 2', ed. The Japanese Society of Calorimetry and Thermal Analysis, Kagakugijutsusha.

10 F. Izumi, 'The Rietveld Methods', Oxford University Press, Oxford 1993, Chap. 13.

11 E. Vila, R. M. Rojas, J. L. Martin de Vidales and O. Garcia-Martinez, Chem. Mater., 8 (1996) 1078.

12 J. L. Martin de Vidales, E. Vila, R. M. Rojas and O. Garcia-Martinez, Chem. Mater., 7 (1995) 1716.

13 C. Cristiani, M. Bellotto, P. Forzatti and E. Tronconi, Appl. Catal., 56 (1990) 253.

14 M. Hosoya, H. Ikuta and M. Wakihara, Solid State Ionics, 111 (1998) 193.